Effects of halide anions on the electrical conductivity in single-crystalline tetra-*n*-butylammonium salt semiclathrate hydrates

Jin Shimada[1,2,3], Takeshi Sugahara[1,2,*], Atsushi Tani[4,5,*], Takahiro Ueda[6], Riko Tsugaya[1,2], Katsuhiko Tsunashima[7], Takayuki Hirai[1,2]

[1]Division of Chemical Engineering, Department of Materials Engineering Science, Graduate School of Engineering Science, Osaka University, 1-3 Machikaneyama, Toyonaka, Osaka 560-8531, Japan

[2]Division of Energy and Photochemical Engineering, Research Center for Solar Energy Chemistry, Graduate School of Engineering Science, Osaka University, 1-3 Machikaneyama, Toyonaka, Osaka 560-8531, Japan

[3]Research Fellow of Japan Society for the Promotion of Science, 5-3-1 Kojimachi, Chiyoda-ku, Tokyo 102-0083, Japan

[4]Department of Human Environmental Science, Graduate School of Human Development and Environment, Kobe University, 3-11 Tsurukabuto, Nada, Kobe, Hyogo 657-8501, Japan

[5]Divison of Terahertz Molecular Chemistry Laboratory, Molecular Photoscience Research Center, Kobe University, 1-1 Rokkodai, Nada, Kobe, Hyogo 657-8501, Japan

[6]Department of Chemistry, Graduate School of Science, Osaka University, 1-1 Machikaneyama, Toyonaka, Osaka 560-8531, Japan

[7]Department of Applied Chemistry and Biochemistry, National Institute of Technology,

Wakayama College, 77 Noshima, Nada, Gobo, Wakayama 644-0023, Japan

Corresponding Authors

*(T.S.) E-mail: sugahara@cheng.es.osaka-u.ac.jp

*(A.T.) E-mail: tani@carp.kobe-u.ac.jp

ORCID

Jin Shimada: 0000-0002-9720-5963

Takeshi Sugahara: 0000-0002-5236-5605

Atsushi Tani: 0000-0001-5788-2137

Takahiro Ueda: 0000-0003-4390-4109

Katsuhiko Tsunashima: 0000-0002-4563-351X

Takayuki Hirai: 0000-0003-4747-4919

KEYWORDS. Semiclathrate hydrate, Electrical conductivity, Water reorientation, Proton conduction, Halide anion

ABSTRACT

Semiclathrate hydrate is an electroconductive material for a possible solid electrolyte and is also useful for monitoring of their formation and dissociation processes. In the present study, the electrical conductivities and electrical relaxation times in the single-crystalline tetra-*n*-butylammonium (TBA) chloride and fluoride semiclathrate hydrates were measured and compared with those of the TBA-bromide semiclathrate hydrate. In descending order of the electrical conductivity, the largest was TBA-bromide semiclathrate hydrate, followed by TBA-chloride and TBA-fluoride semiclathrate hydrates. On the other hand, ^{2}H NMR spin-lattice relaxation times in their deuterates were similar. Although the reorientation motion of water molecules should be a significant factor to govern the electrical conductivity in these semiclathrate hydrates, the present results reveal that the difference between the electrical conductivities in three TBA-halide semiclathrate hydrates would be caused by the concentration of the proton, a conduction carrier, rather than the diffusion processes. Additionally, an electrical conductivity in the single-crystalline TBA-hydroxide semiclathrate hydrate was measured. The electrical conductivity even in single crystal was much higher than those in the TBA-halide semiclathrate hydrates.

1. Introduction

Some clathrate hydrates known as “semiclathrate hydrates (or ionic clathrate hydrates)” show an electrical conductivity higher than that in ice Ih[1-4]. Semiclathrate hydrate is a crystalline inclusion compound made of water molecules with an appropriate quaternary alkyl-onium salt. The water molecules form cage structures, in which the guest cations are encapsulated[5-7]. Some water molecules are replaced with the counter anions. Semiclathrate hydrate is a promising candidate for thermal storage and gas separation media[7,8]. And then, semiclathrate hydrate is a possible solid electrolyte because of its higher electrical conductivity. It seems likely to be used in sensing and monitoring technologies. Recently, we revealed that the proton is a conduction carrier in the tetra-*n*-butylammonium bromide (TBA-Br) semiclathrate hydrate[4]. The electrical conductivity and electrical relaxation time in the TBA-Br semiclathrate hydrate are 4.1×10^{-6} S/cm and 12 μs at 273 K, respectively[4].

As the representative guest ions for semiclathrate hydrates, tetra-*n*-butylammonium bromide (TBA-Br)[5,9,10], chloride (TBA-Cl)[10-12], fluoride (TBA-F)[13,14], and hydroxide (TBA-OH)[15] have been regarded. These guest substances affect the physicochemical properties of semiclathrate hydrates. For example, the phase change temperature and enthalpy are the most important factors for a thermal storage material. It is expected to

be used as a refrigerant suitable for the intended use, e.g., storage of perishable food[16], preservation of vaccines[17,18], and cooling of lithium-ion batteries[19].

The electrical (proton) conductivity in semiclathrate hydrates also would depend on the guest ions. In fact, it was reported that the electrical conductivity in polycrystalline TBA-Br, TBA-Cl, TBA-F, and TBA-OH semiclathrate hydrates depends on the anion species[20-27]. The electrical conductivity in a polycrystalline semiclathrate hydrate is very complicated due to the grain boundaries, quasi-liquid layers, and metastable phases. Therefore, to develop a novel proton conductor or to facilitate the monitoring methodology, it is necessary to understand the proton conduction mechanism in various single-crystalline semiclathrate hydrates. However, the electrical conductivity in single-crystalline semiclathrate hydrates with different ions has never been reported.

In the present study, to reveal the effects of the halide anion on the electrical conductivity in semiclathrate hydrates, we measured the electrical conductivities and electrical relaxation times in the TBA-Cl and TBA-F semiclathrate hydrates by electrochemical impedance spectroscopy (EIS). We used single-crystalline semiclathrate hydrates as experimental samples, as shown in Figure 1, to avoid both the effects of grain boundaries and metastable phases. Additionally, an electrical conductivity in the single-crystalline TBA-OH semiclathrate hydrate was measured for comparison with

those in the TBA-halide semiclathrate hydrates.

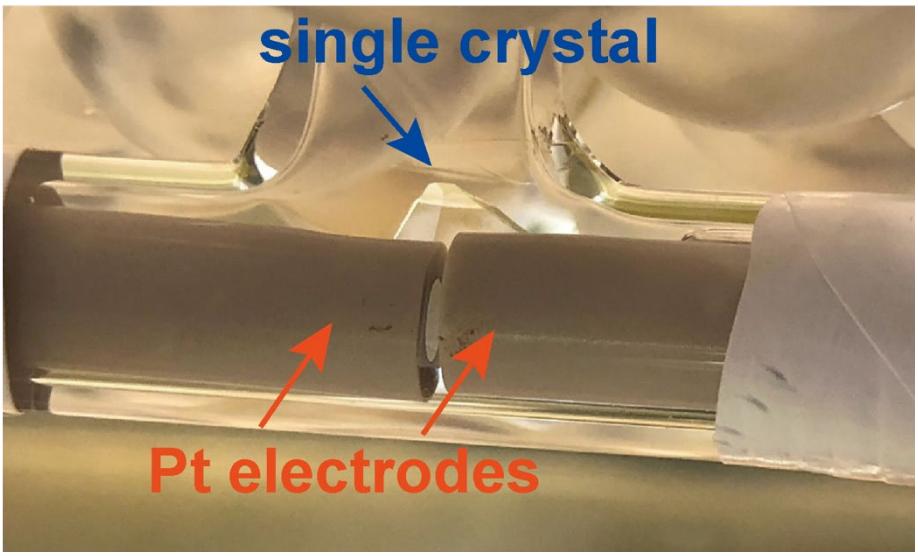

Figure 1. Typical photo of single-crystalline TBA-F semiclathrate hydrate formed between Pt electrodes. The surfaces of both electrodes were completely covered with a single crystal.

2. Experimental

2.1. Samples

Research grade TBA-Cl (Nacalai Tesque Inc., minimum purity of 95 wt%), TBA-F (non-clathrate) hydrate (Tokyo Chemical Industrial Co., Ltd., minimum purity of 98 wt%, mass fraction of TBA-F in the TBA-F hydrate was 0.839), and TBA-OH aqueous

solution (Tokyo Chemical Industrial Co., Ltd., mass fraction of TBA-OH in the aqueous solution was 0.415) were used as semiclathrate hydrate formers. The original water contents of the regents were taken into consideration in the sample preparation. Distilled water was obtained from FUJIFILM Wako Pure Chemical Corporation (resistivity: 0.46 MΩ·cm). For the preparation of the single-crystalline TBA-Cl and TBA-F semiclathrate hydrates, the TBA-Cl (34.18 wt%) and TBA-F (34.13 wt%) aqueous solutions were prepared, respectively. Each mass fraction is very close to the stoichiometric composition of TBA-Cl·30H_2O and TBA-F·28H_2O, respectively[28]. The detailed information of the TBA-OH semiclathrate hydrate will be described later. For a nuclear magnetic resonance (NMR) measurement, TBA-Cl and TBA-F semiclathrate deuterates were prepared using D_2O with minimum purity of 99.9 atomic%, which was obtained from Cambridge Isotope Laboratories, Inc. The effect of H_2O, originally included in the TBA-F reagent, on the NMR result could be negligible because the relative ratio of H_2O to D_2O in the NMR sample was small. Since the effect of H_2O in the TBA-OH regent cannot be ignored, we did not carry out the NMR measurement in the TBA-OH semiclathrate deuterate system.

2.2. Apparatus and procedure

The experimental apparatus and procedure for the electrical impedance measurement are the same as the ones reported previously[4]. Approximately 1 cm^3 of the aqueous solution was poured in an electrochemical measurement cell, which was fabricated from a pair of Pt disk electrodes (electrode area: 0.283 cm^2, distance between electrodes: 1.0 mm) with glass T-tube (VIDTEC)[4]. The cells were immersed in the propylene glycol solution kept at a temperature slightly lower (0.2–0.3 K) than the equilibrium temperature of each semiclathrate hydrate for preparation of single-crystalline semiclathrate hydrates. A seed crystal of each semiclathrate hydrate, grown in another vials, was added into the corresponding aqueous solution to grow single crystals. After a transparent crystal without grain boundaries was prepared at the space between electrodes, the temperature was gradually decreased at a rate of 0.1 K/h and kept constant for over half an hour prior to impedance measurement.

Electrochemical impedance in semiclathrate hydrates was investigated by impedance analyzers (SP-150, Bio-Logic Sciences Instruments Ltd., and Hz-Pro S4, Hokuto Denko Co., Ltd.) in a frequency range from 1 Hz to 1 MHz. The 300 mV of sinusoidal signal (peak-to-peak amplitude) was applied. The impedance results were calibrated with the cell constant obtained in 0.1 M KCl aqueous solution.

The impedance data in TBA-Cl and TBA-F semiclathrate hydrate systems were analyzed with a following equivalent circuit (1)[4]:

$$Z = \frac{R_{\mathrm{hyd}}}{1 + (j\omega)^{p_{\mathrm{hyd}}} R_{\mathrm{hyd}} Q_{\mathrm{hyd}}} + \frac{1}{(j\omega)^{p_{\mathrm{dl}}} Q_{\mathrm{dl}}} \quad (1)$$

where, Z, R, j, ω, p, and Q are impedance, resistance, imaginary unit, angular frequency, fractional exponent of constant phase element, and coefficient of constant phase element, respectively. The subscripts hyd and dl correspond to semiclathrate hydrate and electric double-layer, respectively. The equivalent circuit (1) was applied in the TBA-Br semiclathrate hydrate system we reported previously[4]. Capacitance (C), electrical conductivity (σ), electrical relaxation time (τ), and relative permittivity (ε_r) were estimated from the obtained parameters in equivalent circuits as described in ref. 4.

Solid-state ^{2}H NMR was conducted using AVANCE 400 (Bruker) equipped by a superconducting magnet with the magnetic field of 9.4 T, which corresponds to the resonance frequency of 61.441 MHz for ^{2}H nuclei. Each semiclathrate deuterate was formed around 250 K and was annealed at temperatures slightly lower than the equilibrium temperatures in NMR sample tubes to avoid the coexistence of metastable phases. The spin-lattice relaxation time (T_1) was measured using inversion recovery

[180° – t – 90°] method. The pulse length of 90° and 180° pulses were 5 μs and 10 μs, respectively.

3. RESULTS AND DISCUSSION

3.1. Nyquist plots of EIS for TBA-Br, TBA-Cl and TBA-F semiclathrate hydrates

Figure 2 shows the Nyquist plots of EIS for (Pt | SCH | Pt) cell, where the SCH represents the single-crystalline TBA-Br[4] (measured at 278.2 K), TBA-Cl (at 278.2 K), and TBA-F (at 293.2 K) semiclathrate hydrates. A high-frequency arc and a low-frequency tail were observed. Due to the difficulty of electrochemical impedance measurement in TBA-F semiclathrate hydrate at 278.2 K, we used the results at 293.2 K exclusively for TBA-F semiclathrate hydrate. If we could measure the electrochemical impedance in TBA-F semiclathrate hydrate at 278.2 K, the diameter of arc would be larger than that of 293.2 K. Since the semiclathrate hydrates used in the present study were a single crystal without grain boundaries between the electrodes, neither impedance derived from a metastable phase nor grain boundaries were included.

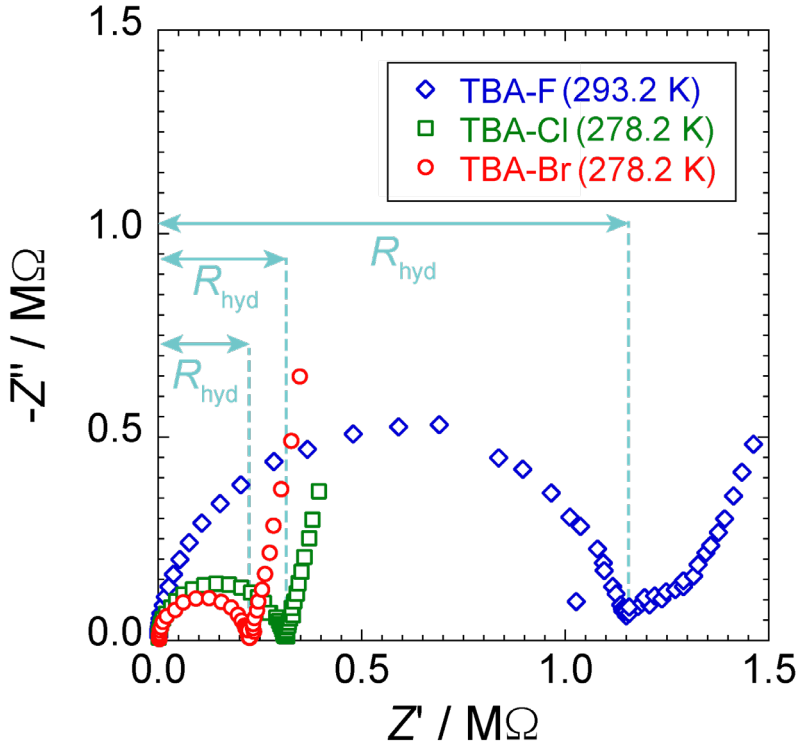

Figure 2. Nyquist plots of (Pt | SCH | Pt) cells measured at 278.2 K (only TBA-F semiclathrate hydrate was measured at 293.2 K) in the single-crystalline TBA-Br[4], TBA-Cl, and TBA-F semiclathrate hydrates (electrode area: 0.283 cm^2, distance between electrodes: 1.0 mm).

3.2. Electrical conductivity in TBA-Br, TBA-Cl, and TBA-F semiclathrate hydrates

Figure 3 shows the temperature dependences (Arrhenius plots) of electrical conductivity in the single-crystalline TBA-Br, TBA-Cl, and TBA-F semiclathrate hydrates. The electrical conductivities exhibited Arrhenius behavior in all the semiclathrate hydrate systems measured in the present study. The obtained values of electrical conductivity (σ) and activation energy (E_σ) are listed in Table 1. The descending order of the electrical conductivities was TBA-Br > TBA-Cl >> TBA-F semiclathrate hydrates. The order of activation energies was TBA-F > TBA-Cl > TBA-Br semiclathrate hydrates. The reported values of electrical conductivity and activation energy in the polycrystalline TBA-Br, TBA-Cl, and TBA-F semiclathrate hydrates[21,22] are also summarized in Table 1. Comparing the results (single crystals) obtained in the present study with those (polycrystals) in references, both the electrical conductivity and the activation energy obtained in the present study were higher (or larger) than those in the references. The reason why the differences emerged should originate from the quality of crystals; for example, polycrystalline semiclathrate hydrates contain grain boundaries, quasi-liquid layer, or metastable phases. Regarding the difference among anions, Opallo et al.[21] suggested that the dependence of electrical conductivity on anion

species may be derived from anion participation in the conduction process: the anion may be a charge carrier or interact with mobile protons. The results we previously reported in the kinetic isotope experiment[4] revealed that the conduction carriers are protons, not anion species, unlike the role of anion as a conduction carrier speculated by Opallo et al.[21] How anions affect the electrical conductivity will be discussed later.

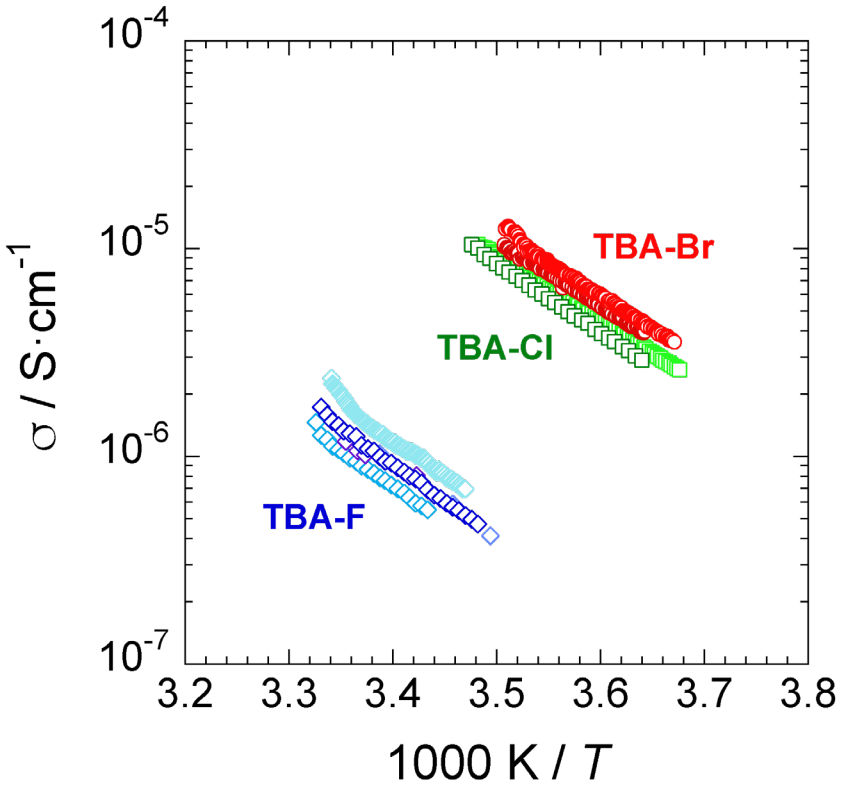

Figure 3. Arrhenius plots of the electrical conductivity in single-crystalline TBA-Br (red circles)[4], TBA-Cl (green squares), and TBA-F (blue diamonds) semiclathrate hydrates. Each sample was measured several times as shown by the symbols with slightly different colors.

Table 1. Electrical conductivity (σ) measured at each temperature (*T*) and estimated activation energy (E_σ) in TBA-Br, TBA-Cl, and TBA-F semiclathrate hydrates.

compound	σ / S·cm^{-1}	E_σ / kJ·mol^{-1}	Ref.
	single crystal		
TBA-Br·26H_2O	4.1×10^{-6} (at 273.2 K)	60.5±0.3	[4]
TBA-Cl·30H_2O	2.6×10^{-6} (at 273.2 K)	61.1±0.3	present study
TBA-F·28H_2O	8.3×10^{-7} (at 293.2 K)	66.0±0.8	present study
	polycrystal		
TBA-Br·32H_2O	1.8×10^{-6} (at 250 K)	43±3	[21]
TBA-Cl·30H_2O	1.7×10^{-8} (at 250 K)	53±4	[21]
TBA-F·32H_2O	1.0×10^{-9} (at 250 K)	50±4	[21]

3.3. Electrical relaxation time and relative permittivity in TBA-Br, TBA-Cl, and TBA-F semiclathrate hydrates

Figure 4 shows the temperature dependence of the electrical relaxation times in the TBA-Br, TBA-Cl, and TBA-F semiclathrate hydrates. The obtained electrical relaxation time and the estimated activation energy in each semiclathrate hydrate are listed in Table 2.

The electrical relaxation time in the TBA-Cl semiclathrate hydrate was almost the same or slightly longer than that in the TBA-Br semiclathrate hydrate. Electrical relaxation time in the TBA-F semiclathrate hydrate was much longer than that in the TBA-Br and TBA-Cl ones.

Additionally, the relative permittivity at the top of frequency in the Nyquist plot of each single-crystalline semiclathrate hydrate was estimated. Relative permittivity (ε_r) was estimated by following equation (2)–(4):

$$C = Q^{\frac{1}{p}} R^{\frac{1-p}{p}} \tag{2}$$

$$C = \varepsilon_s \frac{A}{d} \tag{3}$$

$$\varepsilon_r = \frac{\varepsilon_s}{\varepsilon_0} \tag{4}$$

where, ε_s and ε_0 are permittivity of sample and vacuum, respectively.

It was located at 130–140 for the TBA-Br semiclathrate hydrate[4], 150–160 for the TBA-Cl semiclathrate hydrate, and 160–190 for the TBA-F semiclathrate hydrate in each experimental temperature range.

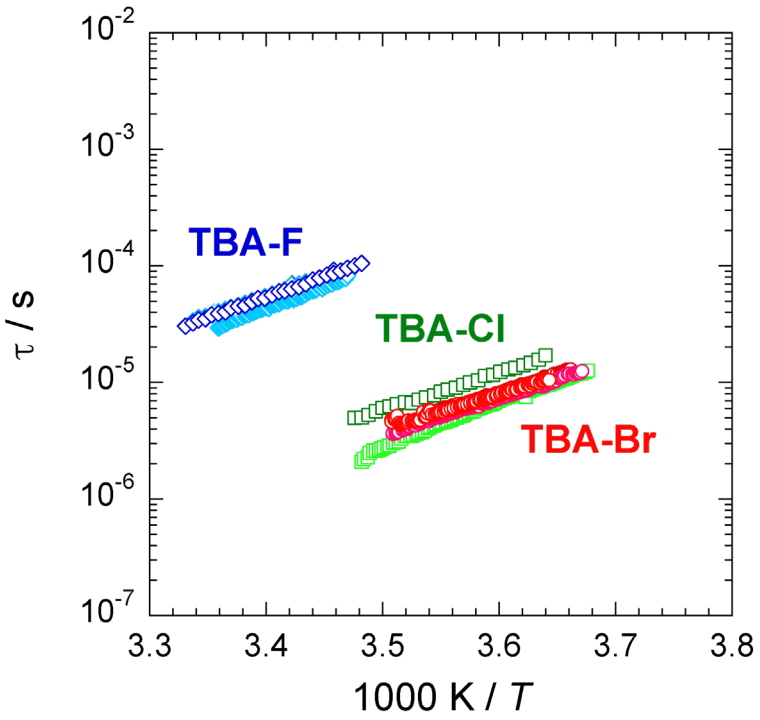

Figure 4. Arrhenius plots of the electrical relaxation time in single-crystalline TBA-Br (red circles), TBA-Cl (green squares), and TBA-F (blue diamonds) semiclathrate hydrates. Each sample was measured several times as shown by the symbols with slightly different colors.

Table 2. Electrical relaxation time (τ) measured at temperature (*T*) and estimated activation energy (E_τ) in the single-crystalline TBA-Br, TBA-Cl, and TBA-F semiclathrate hydrates.

compound	τ / μs	E_τ / kJ·mol^{-1}	Ref.
TBA-Br·26H_2O	12±2 (at 273.2 K)	59.7±0.4	[4]
TBA-Cl·30H_2O	20±6 (at 273.2 K)	63.8±1.1	present study
TBA-F·28H_2O	59±11 (at 293.2 K)	60.9±0.7	present study

3.4. Factors to determine the electrical conductivity in semiclathrate hydrates

The electrical conductivity (σ) with a single carrier is represented by the Nernst-Einstein equation as an equation (5).

$$\sigma = \frac{Dce^2}{kT} \tag{5}$$

D and *c* represent the diffusion coefficient and concentration of charge carrier. The *e*, *k*, and *T* are charge number, Boltzmann constant, and temperature, respectively. From equation (5), to determine the electrical conductivity, we need to estimate the diffusion coefficient *D* and the concentration *c* of charge carrier besides the temperature. The kinetic isotope experiment using the TBA-Br semiclathrate hydrate[4] revealed that the charge carrier in semiclathrate hydrates is the proton (H^+). To elucidate the proton conduction mechanism in the semiclathrate hydrates, it is necessary to comprehend

how large the diffusion coefficient of protons in semiclathrate hydrates is and how many protons generate in semiclathrate hydrates.

As a possible technique to estimate the apparent diffusion coefficient of proton in the semiclathrate hydrates, there might be a solid-state ^{1}H pulse-field gradient NMR (PFG-NMR) measurement. Unfortunately, we cannot access the solid-state PFG-NMR that can measure such a fast diffusion. Alternatively, we measured a solid-state ^{2}H NMR to help understand the dynamics of the water molecules in the semiclathrate hydrates. In the case of clathrate hydrates or ices, it has been considered that the water dynamics, especially reorientation motion, often plays a key role in proton diffusion[1,4,29]. At Bjerrum defects, proton diffusion is temporarily suspended. In order to restart the proton diffusion, the reorientation of the water molecules (alleviation of Bjerrum defects) is necessary. In other words, the reorientation of water molecules is a rate-limiting step of proton diffusion[29]. Such jump of protons between the water molecules can be described by Einstein-Smoluchowski's equation (6)

$$D = \frac{\lambda^2}{2\tau_j} \tag{6}$$

where λ and τ_j represent jump distance and mean residence time of proton, respectively. As we described, water reorientation is a rate-limiting step, suggesting that the τ_j is close to the water reorientation time. Thus, to reveal the proton conduction mechanism

in the semiclathrate hydrates clearly, understanding of the water reorientation motion in the semiclathrate hydrates is essential. The water reorientation time in TBA-Br semiclathrate deuterate was measured and was approximately 0.5 μs[30] or 12 μs[4] at 273 K determined by NMR and/or dielectric measurement. In fact, the water reorientation time of 12 μs is in good agreement with the electrical relaxation time obtained by EIS measurement[4].

The representative line shapes of TBA-Br, -Cl, and -F semiclathrate deuterates recorded by the single pulse sequence was shown in supporting information. The peaks originated from the fast isotopic reorientation motion of D_2O molecules were observed. Figure 5 shows the temperature dependence of the spin-lattice relaxation times (T_1) in the TBA-Br, TBA-Cl, and TBA-F semiclathrate deuterates. Although T_1 was a slightly different among the TBA-halide semiclathrate deuterate systems at 263 K, the values were similar within the range from 243-293 K. In other words, the difference of electrical conductivity in the semiclathrate hydrates would not be caused by the difference in water reorientation time.

The estimated activation energy of T_1 (E_{T1}) is summarized in Table 3. E_{T1} in the TBA-Br, TBA-Cl, and TBA-F semiclathrate hydrates were similar to one another, which were smaller than those of electrical conductivity (E_a). This is because the E_a is due to not

only the reorientation motion of water molecules, but also the formation energy of ion defects, the interaction energy between ions, and the activation energy of proton diffusion, etc.

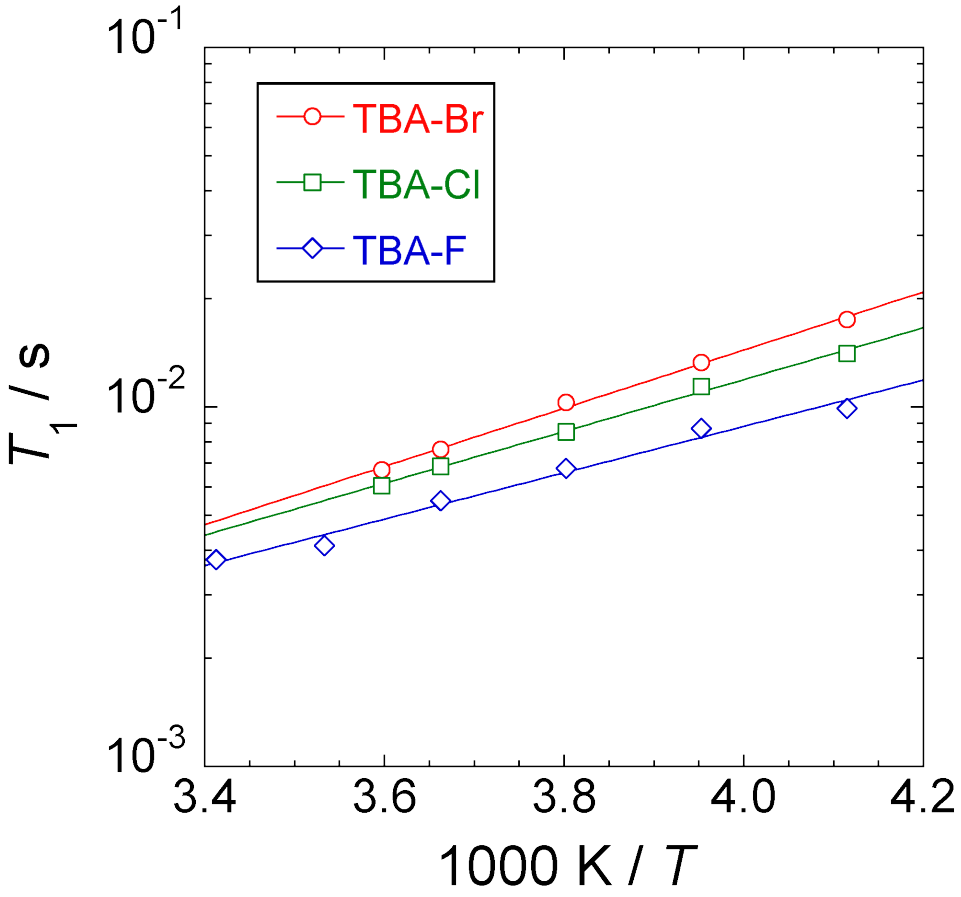

Figure 5. Temperature dependence of spin-lattice relaxation times (T_1) in TBA-Br (red circles), TBA-Cl (green squares) and TBA-F (blue diamonds) semiclathrate deuterates.

Table 3. The estimated activation energy (E_{T1}) of spin-lattice relaxation times (T_1) in TBA-Br[4], TBA-Cl, and TBA-F semiclathrate hydrates.

compound	E_{T1} / kJ·mol^{-1}
TBA-Br·26H_2O	16±1
TBA-Cl·30H_2O	14±1
TBA-F·28H_2O	12±1

The NMR results suggested that the T_1 in the TBA-halide semiclathrate deuterates, which is related to the water reorientation time, was similar. This result supports that the diffusion coefficient (D) of proton in the TBA-halide semiclathrate deuterates is almost the same. On the other hand, the simple Arrhenius plots in the Figure 3 provides us that the thermal process in proton conductions should be simple (possibly single) and other processes could be ignored in these temperature regions. Consequently, we considered that the dominant factor to determine the electrical conductivity in these semiclathrate hydrates would be the concentration of the proton. The electronegativity of halide anions would affect the concentration of the induced carrier. Unfortunately, it is extremely difficult to directly measure the proton concentration or concentration of ionic defects (H_3O^+ and OH^-) in a single-crystalline semiclathrate hydrate. The amount of ionic defects in semiclathrate hydrate should affect the amount of carriers, resulting

in the magnitude of electrical conductivity. This assumption would be qualitatively supported by high electrical conductivities observed in HPF_6[31] and tetramethylammonium hydroxide[20] clathrate hydrates, because they have high concentration of H_3O^+ and OH^- in their aqueous solutions.

Regardless, NMR measurements suggest a conclusion that the electrical conductivity in the TBA-Br, TBA-Cl, and TBA-F semiclathrate hydrates depends on the proton concentration in semiclathrate hydrate crystals, not the diffusion coefficient of proton.

3.5. Electrical conductivity in TBA-OH semiclathrate hydrate

TBA-OH is also a familiar salt for semiclathrate hydrate formation. We measured the electrical conductivity in the single-crystalline TBA-OH semiclathrate hydrate ($TBAOH \cdot 28H_2O$[28]). TBA-OH semiclathrate hydrate was prepared from the aqueous solution with 33.72 wt%.

Representative Nyquist plots of EIS for (Pt | TBA-OH SCH | Pt) cell measured at 278.2 K are shown in Figure 6. Since the capacitance of the TBA-OH semiclathrate

hydrate was much smaller or close to zero, equivalent circuit (7) was applied for the data analysis in the TBA-OH semiclathrate hydrate system.

$$Z = R_{\mathrm{hyd}} + \frac{1}{(j\omega)^{p_{\mathrm{dl}}} Q_{\mathrm{dl}}} \tag{7}$$

The electrical conductivity in the TBA-OH semiclathrate hydrate was 2.0×10^{-2} S·cm^{-1} at 273.3 K, which was much higher than that in the TBA-Br, TBA-Cl, and TBA-F semiclathrate hydrates as shown in Figure 7. Since the electrical conductivity in the TBA-OH semiclathrate hydrate exceeds 10^{-2} S·cm^{-1}, TBA-OH semiclathrate hydrate is classified as a superionic conductor. This trend was consistent with that in a polycrystalline semiclathrate hydrate system. The electrical conductivity in a polycrystalline TBA-OH semiclathrate hydrate was reported to be 10^{-5} S·cm^{-1} at 250 K[22]. Such higher electrical conductivity would be caused by the existence of the OH^- anion[22].

The activation energy of electrical conductivity in the TBA-OH semiclathrate hydrate was 17 kJ·mol^{-1}, which was much smaller than those in the TBA-Br, TBA-Cl, and TBA-F semiclathrate hydrates (approximately 60 kJ·mol^{-1}). This result implies that the proton conduction mechanism would be different from that in the TBA-Br, TBA-Cl, and TBA-F semiclathrate hydrates, although the detailed conduction mechanism is not clear. In

order to clarify the reason of the high electrical conductivity with a small activation energy in the TBA-OH semiclathrate hydrate, further investigation is necessary. Anyway, the discovery of a semiclathrate hydrate with a superionic conductivity, like TBA-OH semiclathrate hydrate, shows the potential for significant development of new solid electrolytes using semiclathrate hydrates. In fact, the electrical conductivity of TBA-OH semiclathrate hydrate is higher than that of α-Li_3PS_4 ($<10^{-3}$ $S \cdot cm^{-1}$ at 298 K)[32] and $Li_7La_3Zr_2O_{12}$ (LLZ) (1.2×10^{-3} $S \cdot cm^{-1}$ at 298 K)[33], which were classified as fast solid electrolytes.

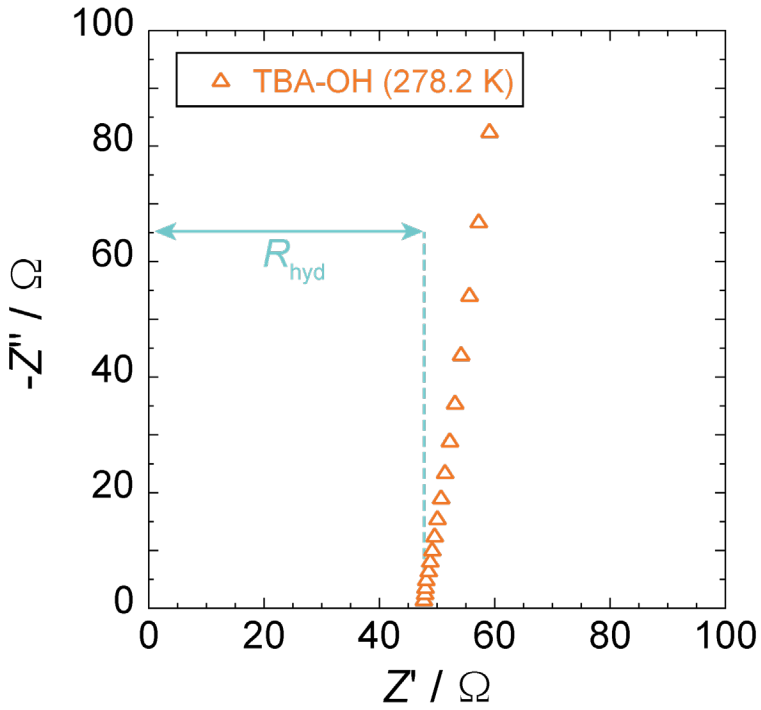

Figure 6. Nyquist plots of (Pt | SCH | Pt) cell measured at 278.2 K in the single-crystalline TBA-OH semiclathrate hydrates (electrode area: 0.283 cm^2, distance between electrodes: 1.0 mm).

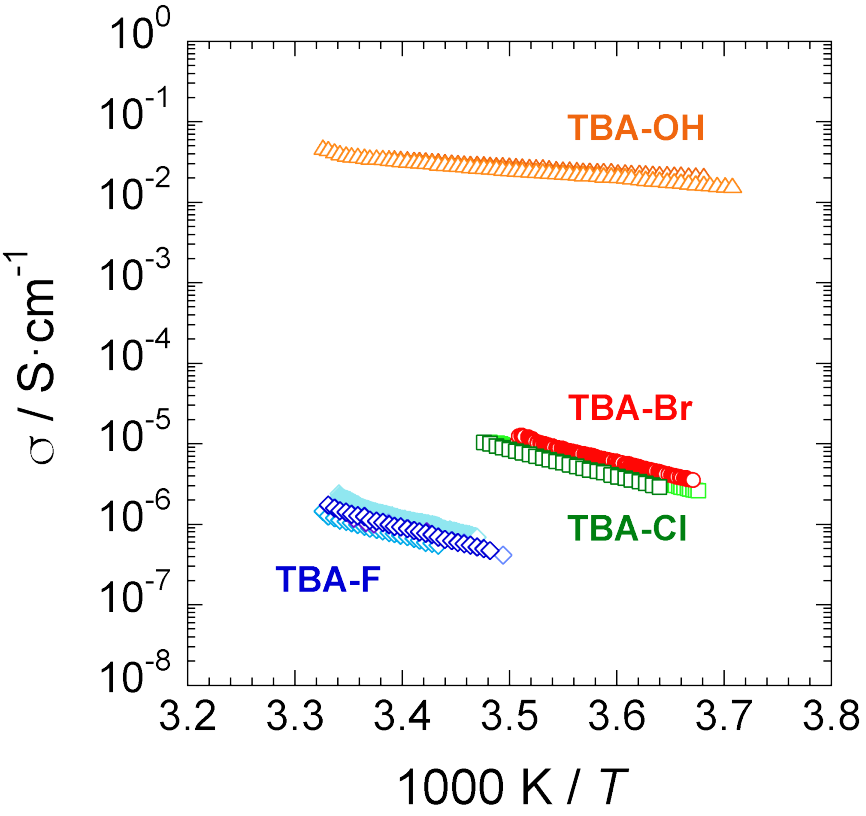

Figure 7. Arrhenius plots of the electrical conductivity in single-crystalline TBA-OH (orange triangles), TBA-Br (red circles)[4], TBA-Cl (green squares), and TBA-F (blue diamonds) semiclathrate hydrates. Each sample was measured several times and the results are shown by the symbols with slightly different colors.

Conclusion

Electrical conductivities and electrical relaxation times in the TBA-Br, TBA-Cl, and TBA-F semiclathrate hydrates were measured. The electrical conductivity decreased in the following order: TBA-Br > TBA-Cl >> TBA-F semiclathrate hydrates. The order of electrical relaxation times in three semiclathrate hydrates was TBA-F > TBA-Cl ≥ TBA-Br semiclathrate hydrates, though the magnitude of order of electrical relaxation times in three semiclathrate hydrates was the same.

According to the Nernst-Einstein equation, the electrical conductivity in the semiclathrate hydrates depends on the diffusion coefficient and concentration of protons besides the temperature. The diffusion coefficient of protons is related to the spin-lattice relaxation time T_1 of water molecules. The T_1 of the D_2O molecules in the TBA-Br, TBA-Cl, and TBA-F semiclathrate deuterates were similar. These results mean that the difference in electrical conductivities results from the proton concentration in the semiclathrate hydrates, which cannot be directly measured.

We believe that the results obtained in the present study will lead to not only the development of semiclathrate hydrates as solid electrolytes but the development of advanced monitoring techniques for semiclathrate hydrate applications.

Acknowledgment

This work was supported by JSPS KAKENHI Grant-in-Aid for JSPS Fellows (JP21J20788 and JP22KJ2069 for JS) and Grand-in-Aid for Scientific Research (JP17H06456 for AT, JP22K05050 for TS, and JP19K05412 for KT). The solid-state NMR measurements were performed at the Analytical Instrument Facility, Graduate School of Science, Osaka University.

Supporting Information

The DSC and ^{1}H NMR results of the semiclathrate hydrates are summarized.

References

1) Du H. Lee, H. Kang, Proton Transport and Related Chemical Processes of Ice, *J. Phys. Chem. B*, 125 (2021) 8270, https://doi.org/10.1021/acs.jpcb.1c04414.

2) J. W. Glen, J. G. Paren, The Electrical Properties of Snow and Ice. *J. Glaciology*, 15 (1975), 15, https://doi.org/10.3189/S0022143000034249.

3) L. A. Stern, S. Lu. R. Constable, W. L. Du Frane, J. J. Roberts, Electrical properties of carbon dioxide hydrate: Implications for monitoring CO_2 in the gas hydrate stability zone, *Geophysical Research Letters*, 48 (2021) e2021GL093475,

https://doi.org/10.1029/2021GL093475

4) J. Shimada, Y. Takaoka, T. Ueda, A. Tani, T. Sugahara, K. Tsunashima, H. Yamada, T. Hirai, Proton conduction in tetra-*n*-butylammonium bromide semiclathrate hydrate, Solid State Ionics, 393 (2023) 116188-1-8, https://doi.org/10.1016/j.ssi.2023.116188.

5) W. Shimada, M. Shiro, H. Kondo, S. Takeya, H. Oyama, T. Ebinuma, H. Narita, Tetra-*n*-butyl-ammonium bromide-water (1/38), *Acta Crystallogr., Sect. C: Cryst. Struct. Commun.*, 61 (2005) o65, https://doi.org/10.1107/S0108270104032743.

6) S. Muromachi, S. Takeya, Y. Yamamoto, R. Ohmura, Characterization of tetra-*n*-butylphosphonium bromide semiclathrate hydrate by crystal structure analysis, *CrystEngComm*, 16 (2014) 2056. https://doi.org/10.1039/C3CE41942H.

7) T. V. Rodionova, I. S. Terekhova, A. Y. Manakov, Ionic Clathrate Hydrates of Tetraalkylammonium/phosphonium Salts: Structures, Properties, Some Applications, and Perspectives, *Energy Fuels*, 36 (2022) 10458, https://doi.org/10.1021/acs.energyfuels.2c01221.

8) Z. Yin, J. Zheng, H. Kim, Y. Seo, P. Linga, Hydrates for cold energy storage and transport: A review, *Advances in Applied Energy*, 2 (2021) 100022, https://doi.org/10.1016/j.adapen.2021.100022.

9) H. Oyama, W. Shimada, T. Ebinuma, Y. Kamata, S. Takeya, T. Uchida, J. Nagao, H.

Narita, Phase diagram, latent heat, and specific heat of TBAB semiclathrate hydrate crystals, *Fluid Phase Equilib.*, 234 (2005) 131, https://doi.org/10.1016/j.fluid.2005.06.005.

10) K. Sato, H. Tokutomi, R. Ohmura, Phase equilibrium of ionic semiclathrate hydrates formed with tetrabutylammonium bromide and tetrabutylammonium chloride, *Fluid Phase Equilibria* 337 (2013) 115– 118 http://dx.doi.org/10.1016/j.fluid.2012.09.016.

11) S. Kim Il-Hyun Baek, J.-K. You, Y. Seo, Guest gas enclathration in tetra-*n*-butyl ammonium chloride (TBAC) semiclathrates: Potential application to natural gas storage and CO_2 capture, *Applied Energy*, 140 (2015) 107, https://doi.org/10.1016/j.apenergy.2014.11.076.

12) T. Rodionova, V. Komarov, G. Villevald, L. Aladko, T. Karpova, A. Manakov, Calorimetric and Structural Studies of Tetrabutylammonium Chloride Ionic Clathrate Hydrates, *J. Phys. Chem. B*,114 (2010) 11838, https://doi.org/10.1021/jp103939q.

13) S. Lee, Y. Lee, S. Park, Y. Seo, Phase Equilibria of Semiclathrate Hydrate for Nitrogen in the Presence of Tetra-*n*-butylammonium Bromide and Fluoride, *J. Chem. Eng. Data*, 55 (2010) 5883, https://doi.org/10.1021/je100886b.

14) J. Sakamoto, S. Hashimoto, T. Tsuda, T. Sugahara, Y. Inoue, K. Ohgaki, Thermodynamic and Raman spectroscopic studies on hydrogen+tetra-*n*-butyl

ammonium fluoride semi-clathrate hydrates, *Chem. Eng. Sci.* 63 (2008) 5789, https://doi.org/10.1016/j.ces.2008.08.026.

15) T. Iwai, S. Takamura, A. Hotta, R. Ohmura, Measurements of the Dissociation Heats of Tetrabutylammonium Acetate and Tetrabutylammonium Hydroxide Ionic Semiclathrate Hydrates, Int. J. Thermophys., 44 (2023) 42, https://doi.org/10.1007/s10765-022-03150-6.

16) X. Xu, X. Zhang, Simulation and experimental investigation of a multi-temperature insulation box with phase change materials for cold storage, *J. Food Eng.*, 292 (2021) 110286, https://doi.org/10.1016/j.jfoodeng.2020.110286.

17) H. Davis, T. Dow, L. Isopi, J.T. Blue, Examination of the effect of agitation on the potency of the Ebola Zaire vaccine rVSVΔG-ZEBOV-GP, Vaccine, 38 (2020) 2643, https://doi.org/10.1016/j.vaccine.2020.02.002.

18) America hospital association, Special Bulletin, COVID-19 vaccine storage requirement, 2022.

19) B. Shabani, M. Biju, Theoretical Modelling Methods for Thermal Management of Batteries, *Energies*, 8, (2015) 10153, https://doi.org/10.3390/en80910153.

20) Z. Borkowska, A. Tymosiak, M. Opallo, Conductivity of stoichiometric $(CH_3)_4NOH$ clathrate hydrates, *J. Electroanal. Chem.,* 406 (1996) 109, https://doi.org/10.1016/0022-

0728(95)04425-6.

21) M. Opallo, A. Tymosiak-Zielinska, Z. Borkowska, Tetra-alkylammonium cation clathrate hydrates as novel proton conductors, *Solid State Ionics*, 97 (1997) 247, https://doi.org/10.1016/S0167-2738(97)00080-5.

22) A. Prokopowicz, M. Opallo, Electrical and electrochemical processes in solid tetrabutylammonium hydroxide hydrate, *Solid State Ionics*, 145 (2001) 407, https://doi.org/10.1016/S0167-2738(01)00937-7.

23) M. Opallo, Z. Borkowska, P. Zoltowski, A. Tymosiak, Electrical Properties of Ionic Conductor below and above Melting Point. Tetraalkylammonium Cation Hydrate, *Solid State Phenomena*, 39 (1994) 321, https://doi.org/10.4028/www.scientific.net/SSP.39-40.321.

24) M. Opallo, A. Tymosiak, Z. Borkowska, Conductivity of tetramethylammonium fluoride tetrahydrate, *J. Electroanal. Chem.*, 387 (1995) 47, https://doi.org/10.1016/0022-0728(95)03859-F.

25) A. Prokopowicz, M. Opallo, Electrochemical hydrogen evolution from solid tetraalkylammonium hydroxide hydrates, *Solid State Ionics*, 157 (2003) 209, https://doi.org/10.1016/S0167-2738(03)00259-5.

26) M. Opallo, A. Prokopowicz, Electrochemical hydrogen evolution in hydroxide

hydrate down to 110 K, *Electrochem. Commum.*, 2 (2000) 23, https://doi.org/10.1016/S1388-2481(99)00134-4.

27) A. Prokopowicz, M. Opallo, Electrochemical hydrogen evolution from solid tetraalkylammonium hydroxide hydrates, *Solid State Ionics*, 162 (2003) 231, https://doi.org/10.1016/S0167-2738(03)00259-5.

28) Y. A. Dyadin, K. A. Udachin, Clathrate polyhydrates of peralkylonium salts and their analogs, *J. Struct. Chem.*, 28 (1987) 394, https://doi.org/10.1007/BF00753818.

29) N. Agmon, The Grotthuss mechanism, *Chem. Phys. Lett.* 244 (1995) 456, https://doi.org/10.1016/0009-2614(95)00905-J.

30) Schildmann, A. Nowaczyk, B. Geil, C. Gainaru, R. Böhmer, Water dynamics on the hydrate lattice of a tetrabutyl ammonium bromide semiclathrate, *J. Chem. Phys*., 130 (2009) 104505, https://doi.org/10.1063/1.3081897.

31) J.-H. Cha, K. Shin, S. Choi, S. Lee, H. Lee, Maximized Proton Conductivity of the HPF_6 Clathrate Hydrate by Structural Transformation, *J. Phys. Chem. C*,112 (2008) 13332, https://doi.org/10.1021/jp805510g.

32) T. Kimura, T. Inaoka, R. Izawa, T. Nakano, C. Hotehama, A. Sakuda, M. Tatsumisago, A. Hayashi, Stabilizing High-Temperature α-Li_3PS_4 by Rapidly Heating the Glass, *J. Am. Chem. Soc*., 145 (2023) 14466, https://doi.org/10.1021/jacs.3c03827.

33) N. Hayashi, K. Watanabe, T. Ohnishi, K. Takada, K. Shimanoe, Impact of intentional composition tuning on the sintering properties of Ca–Bi co-doped $Li_7La_3Zr_2O_{12}$ for co-fired solid-state batteries, *J. Mater. Chem. A*, 11 (2023) 15681, https://doi.org/10.1039/D3TA00921A.

TOC